Intensity and composition-dependent sign reversal of non-linearity in TiO_2/CeO_2 nanocomposites*

S. Divya†, V. P. N. Nampoori, P. Radhakrishnan, and A. Mujeeb

International School of Photonics, Cochin University of Science and Technology, Cochin, Kerala 682022, *India*

(Received 19 June 2013; revised manuscript received 25 July 2013; published online 24 January 2014)

CeO_2/TiO_2 composite nanoparticles with different Ce/Ti molar ratios have been successfully synthesized via sol–gel method. It was found that the band gap of the nanocomposite is tunable by varying Ce/Ti content. The nonlinear response of the sample was studied by using the nanosecond laser pulses from a Q switched Nd:Yag laser employing the *Z*-scan method. Open aperture *Z*-scan experiment revealed that with the increase in the CeO_2 amount in the nanocomposite, the non-linearity of the composite increases, and it was assumed that this could be due to the modification of TiO_2 dipole symmetry by the addition of CeO_2. Closed aperture *Z*-scan experiment showed that when the CeO_2 amount increases, positive nonlinear refraction decreases, and this could be attributed to the increase in the two photon absorption which subsequently suppresses the nonlinear refraction.

Keywords: sol–gel method, non-linearity, *Z*-scan experiment, reversesaturation absorption curve

PACS: 42.65.–k, 42.70.Nq **DOI:** 10.1088/1674-1056/23/3/034209

1. Introduction

Nano-materials with large third-order nonlinear susceptibility $\chi^{(3)}$ and ultrafast response have been under continuous scientific interest because of their potential applications in all-optical switching, light-controlled phase, refractive index modulation, and optical power limiting devices. The nano-materials can be inorganic, organic, or combinations of them. Such nano-scale composite materials containing metal oxides have been continuously focused by the research community for their impending claims in the field of optoelectronic devices. TiO_2 has gained widespread acclaim for its prospective applications such as in dye sensitized solar cells, photo catalysts, gas sensors, electrochromic devices, biomaterials, and so on.[1–4] The large band gap of TiO_2 makes it active only in the UV region, so in order to fruitfully utilize its desirable properties in the visible region, TiO_2 is usually doped with cations or anions or sometimes with other materials with a narrow bandgap.[5–7] CeO_2 is one of the most abundantly found, rare earth compounds which is extensively doped with TiO_2. Ceria-based materials are attractive due to their widespread applications in catalysis, fuel cells, optical films, polishing materials, gas sensors, and other fields.[8] Ce ions are used as activators in various oxide materials for their allowed optical transitions of 4f–5d orbitals. Ce has unique properties because of the availability of Ce^{3+}/Ce^{4+} redox couple and the different optical properties resulting from different electronic configurations, $4f^1 5d^0$ of Ce^{3+} and $4f^0 5d^0$ of Ce^{4+}.[9,10] When nano-TiO_2 is irradiated with ultraviolet (UV) light, an electron is promoted from the valence band to the conduction band, resulting in the generation of energized holes in the valence band. Cerium doping inhibits the recombination rate of electron–hole pairs and thus increases their lifetime.

TiO_2 has a high refractive index and pure TiO_2 also exhibits a fast and reasonably large nonlinear optical response.[11] In this study, CeO_2/TiO_2 composite nanoparticles with different Ce/Ti molar ratios were successfully synthesized via the sol–gel method and its spectral and nonlinear studies were carried out. It was found that the band gap of the nanocomposite can be tuned by varying Ce/Ti content. The nonlinear optical characterization of the TiO_2–CeO_2 nanocomposites was performed by employing open and closed aperture *Z*-scan experiments. This study proved that these nanocomposites belong to the class of materials possessing commendable nonlinear optical (NLO) property.

2. Experiment

The TiO_2–CeO_2 nanocomposites were prepared via the sol–gel method as reported.[12] Here, $CeCl_3{\cdot}7H_2O$ and $Ti(OCH(CH_3)_2)_4$ (titanium butoxide) were used as the precursors for CeO_2 and TiO_2, respectively. $CeCl_3{\cdot}7H_2O$ was dissolved in an adequate amount of ethanol and $Ti(OCH(CH_3)_2)_4$ was added drop wise to the solution. Various percentage compositions have been prepared. Here, t50–c50 means 50% of TiO_2 and 50% of CeO_2 in the nanocomposite.

The prepared samples were characterized by optical absorption measurements using a (JascoV-570) UV/vis/IR spectrophotometer. The nonlinear optical characterization was carried out using *Z*-scan experiment. In this paper, we employed the single beam *Z*-scan technique with nanosecond laser pulses to measure the nonlinear optical absorptive and

*Project supported by the Department of Science and Technology (DST), Govt. of India.

†Corresponding author. E-mail: divyasasi7@gmail.com

© 2014 Chinese Physical Society and IOP Publishing Ltd

refractive properties of TiO_2–CeO_2 nanocomposites. The Z-scan technique developed by Sheik-Bahae *et al.* is a single beam method for measuring the sign and magnitude of nonlinear refractive index n_2, and has a sensitivity comparable to interferometric methods.[13,14] A Q-switched Nd: YAG laser (Spectra Physics LAB-1760, 532 nm, 7 ns, 10 Hz) was used as the light source. The samples to be investigated were mounted on a translation stage controlled by a computer and were moved along the z axis through the focal point of a lens with a focal length of 20 cm. The radius of the beam waist ω_0 was calculated to be 35.4 μm. The Rayleigh length $z_0 = \pi\omega_0^2/\lambda$ was estimated to be 7.4 mm, which was higher than the thickness of the sample. This is an essential prerequisite for Z-scan experiments. The transmitted beam energy, reference beam energy, and their ratio were simultaneously measured by an energy ratiometer (Rj7620, laser probe corp) having two identical pyro electric detector heads (Rjp735). The data were analyzed and the nonlinear coefficients were studied by fitting the experimental Z-scan curve with the theoretical curves.

3. Results and discussion

Optical absorption measurement is an initial step to characterize the nanocomposite. Figure 1 illustrates the absorption spectra of the prepared nanocomposites. Absorption spectroscopy helps to understand the electronic transition of a valence state. It is seen that one broad absorption band appears at around 450 nm in the spectral range from 400 nm to 500 nm. This peak is due to 4f to 5d transition of Ce^{3+}.[15,16] The observed 450-nm peak is due to 4f to 5d transition of Ce^{3+} in the ligand environment of O^{2-} of TiO_2 nanoparticles. Hence, it can be concluded that the Ce^{3+} is the prominent valence state of Ce present on the surface as well as on the core of the TiO_2 nanoparticle. As a result, blue radiation is strongly absorbed by the allowed 4f to 5d transition of Ce^{3+}, emitting yellow.[17] It is observed that as the amount of CeO_2 increases, this band gets blue shifted due to quantum size confinement.

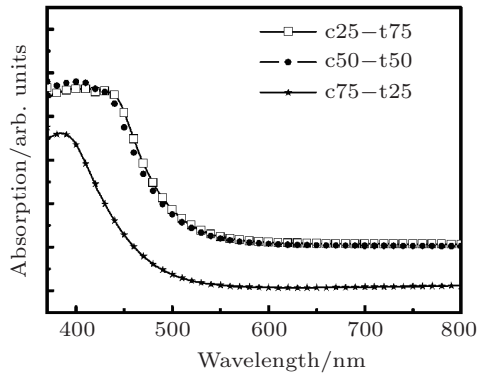


Fig. 1. Absorption (in arbitrary units) versus wavelength for TiO_2/CeO_2 nanocomposites.

Figure 2 represents the band gap calculation of the nanocomposite as per Tauc's plot. The band gap was estimated from the graph of $h\nu$ versus $(\alpha h\nu)^2$ for the absorption coefficient α which is related to the band gap E_g as

$$(\alpha h\nu)^2 = \text{const}\left(h\nu - E_g\right), \tag{1}$$

where $h\nu$ is the incident light energy.

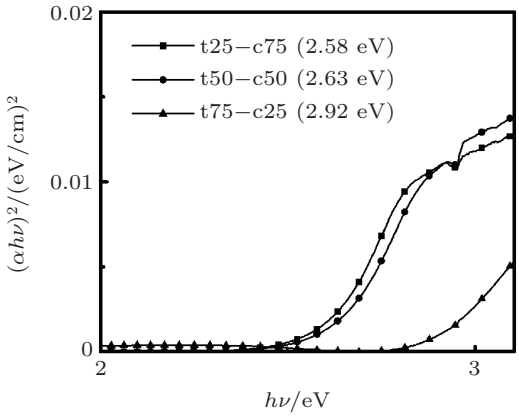


Fig. 2. Band gap estimation of the nanocomposites from Tauc's equation.

It has been observed that as the CeO_2 amount increases, the band gap decreases. The narrowing of the band gap can be due to the formation of Ce 4f and oxygen defect levels which are beneath the conduction band (CB) minimum. The oxygen defects levels are formed while balancing the charge between Ti^{4+} and Ce^{3+}. The localized band states produced by these 4f electrons and oxygen defect levels allow maximum electronic transitions to occur to these levels.[18,19] The localized states of CeO_2 smudges out to the forbidden energy gap of TiO_2 leading to the formation of Urbach tail and the energy associated with it is known as Urbach energy which can be calculated from the expression $\alpha = \alpha_0 \exp(E/E_u)$, where E_u denotes Urbach energy.

For a nonlinear medium, the third-order nonlinear susceptibility is given by $\chi^{(3)} = \chi_R^{(3)} + i\chi_{im}^{(3)}$, where the real part $\chi_R^{(3)}$ is related to the nonlinear index of refraction coefficient n_2 as $\chi_R^{(3)} = 2n_2\varepsilon_0 n_0^2 c$, where $n = n_0 + n_2 I$, and the imaginary part is related to nonlinear absorption coefficient β as $\chi_{im}^{(3)} = \varepsilon_0 n_0^2 c^2 \beta/\omega$, where $\alpha = \alpha_0 + \beta I$, n_0, α_0 are linear refractive index and linear absorption coefficient, n and α refer to the intensity dependent refractive index and intensity dependent absorption coefficient,[20] and β and n_2 are determined by open and closed aperture Z-scan experiments respectively. This experiment also allows the study of the sign of nonlinear refractive index. The normalized transmittance for the open-aperture condition is given as

$$T(z, S=1) = \frac{\int_{-\infty}^{\infty} \ln\left[1 + q_0(z,0)\, e^{-\tau 2}\right] d\tau}{\sqrt{\pi} q_0(z,0)}. \tag{2}$$

Here, $q_0 = \beta I(t) L_{\text{eff}}/(1+z^2/z_0^2)$; $S=1$ symbolises open aperture, where β, γ can be easily found. In case of closed aperture

$$T(z,\Delta\varphi_0) = 1+\frac{4\Delta\varphi_0 x}{(x^2+9)(x^2+1)}. \quad (3)$$

Here, $x = z/z_0$, $\Delta\varphi_0 = 2\pi n_2 I_0 L_{\text{eff}}/\lambda$.

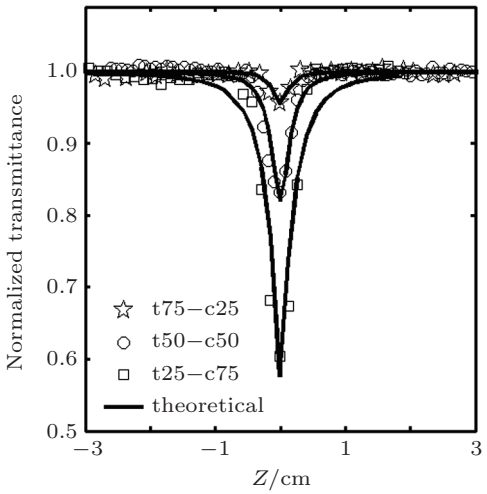


Fig. 3. Open aperture Z-scan of the nanocomposites. The solid curves show the theoretical fitting.

Figure 3 shows the open aperture Z-scan curve of the nanocomposites. It is observed that the graph obtained follows a reverse saturation absorption curve (RSA). Generally, RSA can occur due to two photon absorption (TPA) or free carrier absorption. Two photon absorption is one of the most important nonlinear processes in semiconductors. In addition, TPA dominates as it satisfies the relation $E_g/2 < h\nu < E_g$ here. This result agrees very well with the TPA process reported in bulk TiO_2 samples.[21,22] Ce 4f level and oxygen defects present below the CB edge undergo hybridization to produce an impurity band and it is proposed that this level acts as the intermediate level enabling the two photon absorption as represented in Fig. 4.[23] As the graph very clearly fits the theoretical curve indicated in solid lines, this further confirms the assumption.

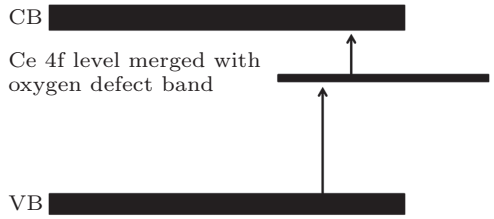


Fig. 4. Energy band diagram of TiO_2:CeO_2, VB and CB correspond to valence band and conduction band, respectively.

In Fig. 3, it can be observed that as the CeO_2 concentration increases, non-linearity also increases as indicated by the dip in the curve. Thus, it can be assumed that Ce^{3+} modifies the local symmetry of TiO_2 thereby enhancing optical non-linearity. It is usually expressed in terms of

$$\beta = \left(2\pi/n_0^2\varepsilon_0 c\lambda\right) \text{Im}\left\{\chi^3\right\}. \quad (4)$$

Figure 5 shows the closed aperture Z-scan curve of the nanoparticle of the composition t75–c25 at the wavelength of 532 nm mentioned above at different laser intensities. Initially, the closed aperture exhibits a peak to valley shape, depicting a negative value of nonlinear refractive index n_2. The theoretical fit to the experimental data is obtained from Eq. (3). In order to obtain the phase distortion caused by the change in refractive index, normalized closed aperture data are divided by the corresponding normalized open aperture data. It is observed that peak–valley of closed aperture Z-scan satisfies the condition $\Delta z \sim 1.7 z_0$ thus confirming the presence of cubic non-linearity.[24]

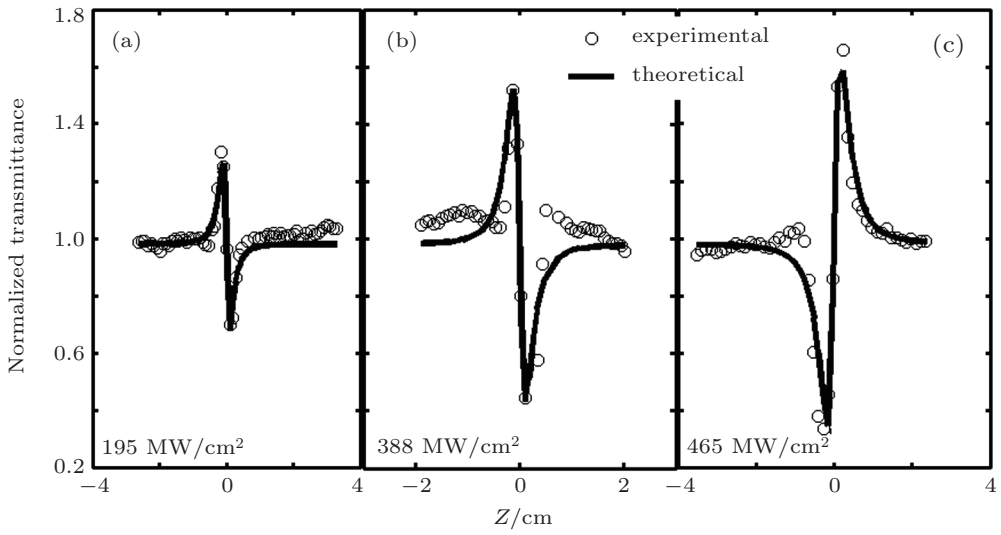


Fig. 5. Closed aperture Z-scan results at different exciting laser intensities: (a) 195 MW/cm^2, (b) 388 MW/cm^2, (c) 465 MW/cm^2. The solid curves show the theoretical fitting.

The ΔT_{p-v} difference between peak and valley is obtained from the theoretical curve. The nonlinear refractive index n_2 and the real part of nonlinear susceptibility $\mathrm{Re}\{\chi\}$ are related as

$$\mathrm{Re}\{\chi\} = 2n_2\varepsilon_0 n_0^2 c, \tag{5}$$

where

$$n_2 = \frac{\Delta T_{p-v}}{0.406(1-s)^{0.25} k L_{\mathrm{eff}} I_0}. \tag{6}$$

The peak–valley trace in closed aperture Z-scan shows that these samples show switching between self-focusing ($n_2 > 0$) and self-defocusing ($n_2 < 0$) non-linearity. From the model suggested by Sheik-Bahae *et al.,* the sign of nonlinear refraction is positive when the photon energy is smaller than $0.7E_g$ where E_g is the band gap of the materials.[25] The n_2 becomes negative when the photon energy is in the range of $0.7E_g$–E_g. In the present case the photon energy is 2.336 eV and hence theoretically all the samples should have negative nonlinear refractive index. However, our results deviate from the proposed model. We suggest that this could be due to the fact that as the power is increased, the concentration of excited electrons increases which increases the nonlinear refraction resulting in self-focusing.[26] Similar switching behavior was also obtained for other compositions. It has been observed that as the amount of CeO_2 increases in the nanocomposite, switching from negative to positive nonlinear refraction occurs at much higher laser power. This intensity-dependent nonlinear refraction described here is expected to have potential applications in optical information processing.

Figure 6 shows the closed aperture Z-scan curve of the nanocomposite of varied composition at the same power (465 MW/cm^2). The corresponding values of n_2 are shown in Table 1. It is observed that as the amount of TiO_2 increases in the composition, nonlinear refraction increases. This can be credited to the fact that as the amount of CeO_2 increases, RSA increases due to enhanced two photon absorption thereby reducing the possibility of positive nonlinear refraction.[27] Thus, by varying the amount of CeO_2 in the nanocomposite switching phenomenon is conceivable, which has potential applications in the field of photonics technology.

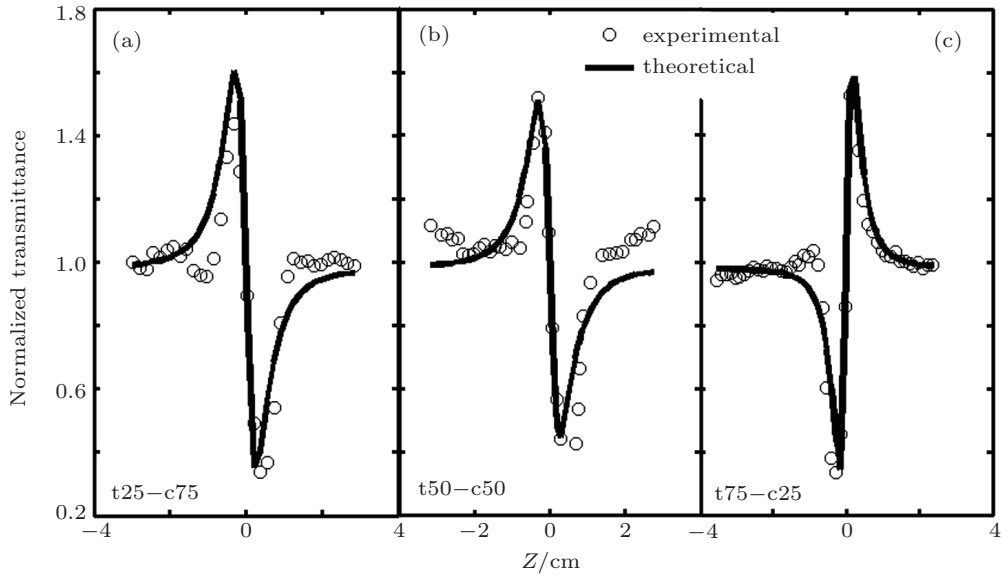


Fig. 6. Closed aperture Z-scan results for different compositions: (a) t25–c75; (b) t50–c50; (c) t75–c25. The solid curves show the theoretical fitting.

Table 1. Various values of $\mathrm{Im}\{\chi\}$ and $\mathrm{Re}\{\chi\}$ of the nanocomposites at 465 MW/cm^2.

Composition of t–c	$\beta \times 10^{-10}$ /(m/W)	$n_2 \times 10^{-17}$ /(m^2/W)	$\mathrm{Im}\{\chi\} \times 10^{-16}$ /(m^2/V^2)	$\mathrm{Re}\{\chi\} \times 10^{-18}$ /(m^2/V^2)
t25–c75	5.18	–6.14	5.37	–1.36
t50–c50	2.65	–5.64	3.26	–1.46
t75–c25	1.64	7.44	2.78	1.66

4. Conclusion

In conclusion, different compositions of TiO_2–CeO_2 were synthesized using the sol–gel method. It is observed that as the dopant concentration increases, the band gap decreases. Nonlinear property of the nanocomposite was also studied using Z-scan apparatus. It was observed that the nanocomposites show admirable non-linearity owing to two photon absorption followed by the modification in the symmetry of TiO_2 dipole due to charge compensation. Nonlinear refractive index of the nanocomposite was also estimated. Variation of the nonlinear index of refraction was studied with respect to power as well as composition. Switching in the sign of nonlinear refractive index occurred in both cases and possible reasons for the same were discussed. Employed experiments proved their imminent application as optical limiters as well as for optical information processing.

References

[1] Sanchez C, Lebeau B, Chaput F and Boilot J P 2003 *Adv. Mater.* **15** 1969

[2] Sanchez C, Soler-Illia G D A, Ribot F, Lalot T, Mayer C R and Cabuil V 2001 *Chem. Mater.* **13** 3061

[3] Novak B M 1993 *Adv. Mater.* **5** 422

[4] Wang Y, Zhang S and Wu X 2004 *Nanotechnology* **15** 1162

[5] Klosek S and Raftery D 2002 *J. Phys. Chem. B* **105** 2815

[6] Yamaki T, Sumita T and Yamamoto S 2002 *J. Mater. Sci. Lett.* **21** 33

[7] Sathish M, Viswanathan B and Viswanath R P 2007 *Appl. Catal. B* **74** 307

[8] Yuan Q, Duan H H, Li L L, Sun L D, Zhang Y W and Yan C H 2009 *J. Colloid Interface Sci.* **151** 335

[9] Orera V M, Merino R I and Pena F 1994 *Solid State Ionics* **72** 224

[10] Choudhury B, Bikash B and Amarjyoti C 2012 *Photochem. Photobiol. A* **31** 1

[11] Long H, Chen A, Yang G, Li Y and Lu P 2009 *Thin Solid Films* **517** 5601

[12] Divya S, Nampoori V P N, Radhakrishnan P and Mujeeb A 2013 *Appl. Phys. A*

[13] Wang X H, Shi J, Dai S and Yang Y 2003 *Thin Solid Films* **429** 102

[14] Yang P, Song C F, Lü M K, Yin X, Zhou G J, Xu D and Yuan D R 2001 *Chem. Phys. Lett.* **345** 429

[15] Li F B, Li X Z, Hou M F, Cheah K W and Choy W C H 2005 *Appl. Catal, A* **285** 181

[16] Xie J, Jiang D, Chen M, Li D, Zhu J, Lu X and Yan C 2010 *Colloids Surf. A* **372** 107

[17] Blasse G, Schipper W and Hamelink J J 1991 *Inorganica Chimica Acta* **189** 77

[18] Fu C, Li T, Qi J, Pan J, Chen S and Cheng C 2010 *Chem. Phys. Lett.* **494** 117

[19] Chen S W, Lee J M, Lu K T, Pao C W, Lee J F, Chan T S and Chen J M 2010 *Appl. Phys. Lett.* **97** 012104

[20] Sheik-Bahae M, Said A A, Wei T H, Hagan D J and van Stryland E W 1990 *IEEE J. Quantum Electron.* **26** 760

[21] Torres-Torres D, Trejo-Valdez M, Castañeda L, Torres-Torres C, Tamayo-Rivera L, Fernández-Hernández R C, Reyes-Esqueda J A, Muñoz-Saldaña J, Rangel-Rojo R and Oliver A 2010 *Opt. Express* **18** 16406

[22] Wang S X, Zhang L D, Su H, Zhang Z P, Li G H, Meng G W, Zhang J, Wang Y W, Fan J C and Gao T 2001 *Phys. Lett. A* **281** 59

[23] Liu T X, Li X Z and Li F B 2010 *Chem. Eng. J.* **157** 475

[24] Sheik-Bahae M, Said A A and van Stryland E W 1989 *Opt. Lett.* **14** 955

[25] Sheik-Bahae M, Hagan D J and van Stryland E W 1990 *Phys. Rev. Lett.* **65** 96

[26] Wang K, Long H, Fu M, Yang G and Lu P X 2010 *Opt. Lett.* **35** 1560

[27] Draine B T and Flatau P J 1994 *J. Opt. Soc. Am. A* **11** 1491